Contrib Mineral Petrol (1985) 91:360–368

Contributions to Mineralogy and Petrology

A new partial substitution mechanism of CO_3^{2-}/CO_3OH^{3-} and SiO_4^{4-} for the PO_4^{3-} group in hydroxyapatite from the Kaiserstuhl alkaline complex (SW-Germany)

J. Sommerauer [1] **and K. Katz-Lehnert** [2]

[1] Institut für Mineralogie und Petrographie (IMP), ETHZ 8092 Zürich, Switzerland
[2] Mineralogisch-petrographisches Institut Universität Freiburg i.Br., Federal Republic of Germany

Abstract. Based on a detailed mineral-chemical investigation of apatite from a series of carbonatites and associated silicate volcanic rocks of the Kaiserstuhl tertiary alkaline volcanic centre, evidence for a new substitution mechanism was found within the hydroxyapatite group, yielding the following simplified formula:
$(Ca, Sr, LREE)_{10}(SiO_4)_x(CO_3)_x(PO_4)_{6-2x}(OH, F)_2$ with $0<x<1.2$
LREE represents light rare-earth elements such as Ce, La, and Nd. Other elements were detected included Cl, S and traces of Mg, Al, K, Fe, Mn, and Th, however they have no effect on the substitution mechanism found. F is present in varying amounts, although well under half of the total possible halogen content (3.7 wt.% F), and shows a distinct antipathetic concentration correlation with REE and Si (and in turn with C). Charge balance is generally maintained by the coupled substitution of CO_3^{2-} and SiO_4^{4-} for PO_4^{3-}; however, excess charge may be subsequently adjusted by CO_3OH^{3-} partly accompanied by the REE in the Ca site.

Introduction

The Kaiserstuhl complex, situated in the upper Rhine graben, exhibit a sequence of volcanic and subvolcanic rocks of miocene age which form part of a wide alkaline igneous activity in SW Germany. The complex comprise highly differentiated phonolitic and tephritic-essexitic subvolcanic intrusives and dykes, lavas and tuffs. A carbonatite body emplaced centrally in the silicate volcanic rocks and numerous carbonatite dykes of several centimeters up to 10 m intruded in the adjacent subvolcanic rocks. The majority of the carbonatite appears as soevitic bodies. Alvikites, porphyritic alvikites and subordinate comb-layer alvikites (Katz and Keller 1981) are found as dykes. Extrusive carbonatite lapillis are structurally similar to the alvikites (Keller 1981). Further details of the petrological setting and rock types are outlined in Wimmenauer (1957, 1959, 1962, 1967) and Katz-Lehnert and Sommerauer (in prep). All these rock types contain idiomorphic accessory apatites of different morphology.

In the course of a detailed mineral-chemical investigation of apatites from selected carbonatites and silicate igneous rocks, characteristic chemical features inherent to all samples analyzed were recorded. The apatites were found to be essentially hydroxyapatite, with low to moderate F concentration. Low F concentration is accompanied by variable but high amounts of Si and C. While there are no reported indications that C and Si occur together as major constituents in apatites, carbonate-bearing apatite and carbonate-apatite (dahlite, francolite) are known to exist in organic materials and marine sediments (Manheim and Gulbrandsen 1979), in phosphorite deposits (Axelrod and Rohrlich 1982), and are not uncommon in igneous and metamorphic rocks (McConnell and Gruner 1940; Gulbrandsen et al. 1966; McClellan and Lehr 1969; Prins 1973). On the other hand, silicon-containing apatite and silicate-apatite (ellestadite, wilkeite) as an essentially carbon-free phase has frequently been described, e.g. by McConnell (1937), Taborsky (1962), Ito (1968), Nash (1972), Rouse and Dunn (1982). Thus, the apatites of the present study which are abundant in both silicon and carbon offer an excellent opportunity for deriving a further substitution mechanisms in apatite.

Up to the present, there has been no detailed crystal-chemical study of the apatite from the various Kaiserstuhl alkaline rocks and associated carbonatite complex. Partial analyses have been reported by Daub (1912) on F concentration, by Van Wambecke (1964) on selected trace elements, and by Puchelt and Emmermann (1976) and Belyakov and Kravchenko (1979) on REE patterns. In order to account for this apparent special type of apatite and to gain more information on the genesis and evolution of the carbonatites in particular (Katz-Lehnert, in prep and Katz-Lehnert and Sommerauer, in prep), a comprehensive survey of the apatite mineralogy was thought to be of interest.

The present investigation is based on extensive electron microprobe analyses together with x-ray diffraction studies on apatite samples from different carbonatitic rock types. Included in the study for comparison purposes were apatites from some associated silicate rock samples. Special attention was given to the acicular apatites from comb-layer alvikite dykes, which feature trapped phosphate melt inclusions. A discussion of this is the topic of a separate study (Sommerauer and Katz-Lehnert 1985).

Materials

Apatite is extensive in all carbonatite rock types as well as in the silicate volcanic rocks in the Kaiserstuhl. The apatite concentration in the silicate rocks ranges from 0.5 to about 1.5 vol.% (Wimmenauer 1963). Its occurrence is extremely variable in the carbonatites, ranging between 1 and

5 vol.% for alvikites and comb-layer alvikites, and averaging 3 vol.% in soevites (Walther 1981). Locally apatite may nevertheless reach up to 10 vol.% (Wimmenauer 1963).

According to the different nature of rock textures in the carbonatites, appreciable variation of grain size and of morphology of the apatites is observed which is obviously controlled by the cooling history of the carbonatite rock types (Katz-Lehnert and Sommerauer, in prep). The grain size may vary from few microns in comb-layer alvikites up to 100 μm in soevites. Acicular habit is characteristic for apatites in comb-layer alvikites, they are needle-like to prismatic in alvikites and porphyric alvikites, and in soevites apatites are generally of short, occasionally long prismatic habit and show abundant primary fluid inclusions studied in detail by Walther (1981). The apatites from the silicate rock types are texturally less extreme and resemble more the crystals from the soevitic carbonatites.

In order to cover the textural range, apatite samples were collected from selected localities described in Katz-Lehnert and Sommerauer (in prep) representing specimens from comb-layer alvikites (samples 11/17 and 837), porphyritic alvikites (samples 11/29, 219, 5/12, and 162.2), from an alvikite s.s. (sample 12/18), soevites (samples 275, 205, and 400.3), and from carbonatite lapillis (samples I and II). For comparison purposes, apatites from a shonkinite porphyry (Horberig), a phonolitic dyke (Boetzingen), a phonolitic tuff (Limberg), a bergalite (sample 217), a cpx-bergalite (sample 430), and from a tephrite dyke (sample 435) were also investigated.

Methods

Heavy liquids were used to separate the apatite from other phases present in the assemblages. These apatite concentrates were carefully washed in acetic acid to achieve apatite samples free of carbonate (especially important for the carbon determination by means of coulometric titration and for DTA-MS measurement). A magnetic separator was used to separate residual magnetite. Finally, the concentrates were upgraded by hand sorting, repeatedly washed in decarbonated water and dried at 60° C. Up to this point no heat treatment was applied.

For the electron microprobe analyses, apatite concentrates were embedded in epoxy mounts, ground and polished. When it was of special interest to study the chemical relationship of apatite to the coexisting minerals, polished thin-sections were prepared.

The chemical characterization is based primarily on detailed electron microprobe analyses of a selection of representative apatite concentrates. Other methods were applied to test and append these results. For the carbon determination, coulometric titration was used. Combined differential thermo-analysis with mass-spectrometry (DTA-MS) and IR spectroscopy served to support the carbon data. It is evident that the results obtained by electron microprobe technique may not be directly compared to the results of the other two methods. Two apatite concentrates were measured by means of neutron activation analysis (NAA) for REE to cross-check the electron microprobe data. This was carried out at the EIR (ETHZ). The chemical results were related to x-ray lattice constant determinations of a selection of apatite concentrates.

Electron microprobe analyses

The apatites were investigated using an automated ARL SEMQ electron microprobe equipped with an x-ray energy analyzer (TN 2000 by Tracor Northern). Five x-ray crystal spectrometers (WDS) and the x-ray energy dispersive system (EDS) were applied simultaneously for quantitative analyses. An acceleration potential of 15 KV with a sample current of 20 to 40 nA (measured on brass) was applied, yielding a minimum beam size of 0.2 μm which was maintained for all measurements. For EDS data collection, integration time was 40 to 120 s per analysis which results in counting statistics better than 0.6% (1 sigma) for the major elements. The WDS under the same excitation conditions gave values better than 0.4% (1 sigma) for minor element concentrations except for F which would reach 20% (1 sigma) at the 1 wt.% level. In special cases time and/or beam current was increased to improve precision. WDS or EDS techniques were selected dependant on the minimum detectable limits (MDL) as required for adequacy of the low level data. The individual MDL values (in wt.%) were: $La_2O_3 < 0.05 >$, $Ce_2O_3 < 0.06 >$, $SrO < 0.06 >$, $Na_2O < 0.04 >$, $K_2O < 0.02 >$, $SiO_2 < 0.14 >$, $SO_3 < 0.04 >$, $F < 0.11 >$, and $Cl < 0.02 >$. Natural and synthetic materials comprising apatites, silicates, aluminates, and oxides were used as standards. Both samples and standards were coated with 200 Å of carbon for the quantitative analyses. For the semi-quantitative determination of C, the samples were coated with 250 Å of Be. On-line correction for dead-time, drift and background (Sommerauer 1981) was applied to the raw data. Full correction for x-ray absorption, atomic number effect, and x-ray fluorescence (by characteristic and continuum excitation) were based on a ZAF program written for the CDC Cyber-700 series computer system at the ETHZ (Gubser and Sommerauer 1977).

Coulometric determination

Apatite concentrates were measured with a Coulomat CS 701, based on coulometric alkalimetric titration (Sixta 1977). Approximately 100 mg of each carefully washed apatite concentrate sample was finely ground. This provided a large reaction surface and in turn good accessibility to possible carbonate inclusions. Generally four independant runs were carried out with/without LiB_4 flux in either O_2 or N_2 atmosphere, heated to 1,250° C with O_2 and to 1,350° C with N_2. Without flux, the temperature was well below the melting point of apatite, in contrast to the admixture of flux. This four-run method permits determination of carbon either as elemental carbon or as CO_2 and indicates which mineral phase carbon should be attributed to. Data precision was 2% relative. The coulometric analyses were carried out at the IMP ETHZ.

Differential thermal analyses with mass-spectrometry (DTA-MS)

Splits of the apatite concentrates as analyzed by the coulometric titration were also investigated by means of a Mettler DTA-MS instrument at the Institut für Kristallographie and Petrographie (IKP) ETHZ. The heating experiments were conducted up to 1,000° C with a heating rate of 10° C/min. In addition to CO_2, the groups SO_2, OH, and HF could also be qualitatively determined.

X-ray diffraction studies

The powder diffraction data were obtained using a Jagodzinski x-ray diffraction camera with filtered $Cu_{K\alpha d}$ radiation. Si was used as an internal standard. All of the recorded diffraction lines could be positively indexed with respect to the ASTM powder data file. Refinement of the lattice constants was based on 22 to 35 powder lines. The lattice constants were computed by a one-pass noniterative least-square method which provided reciprocal tensors and its variance-covariance matrix.

IR-spectroscopy

Splits (4 mg) of the powdered apatite concentrates were mixed with 300 mg KBr and pressed to form pills. These were analyzed using a Perkin Elmer grating IR spectroscopic instrument PE mod 457 at the IKP ETHZ. The apatite reference standards G004 and G005, as well as the samples 11/17, 5/12, and 11/29 were studied. Special attention to the O−H vibration at 3,540 cm^{-1}, the C−H vibration at 2,930 cm^{-1}, and the C−O vibration splitting to 1,470 and

Table 1a. Electron microprobe analyses of apatites from various carbonatite rock types. Mean and standard deviations

	Soevites		Alvikites				Lapillis		Comb-layer alvikites		Trapped melt inclusions in 11/17 [7]
	400.3 [6]	205 [13]	Porph. 11/29 [12]	Porph. 5/12 [21]	Porph. 162.2 [9]	s.s. 12/18 [3]	I [6]	II [1]	837 [15]	11/17 [23]	
CaO	53.5 (5)	54.1 (4)	53.3 (6)	53.6 (4)	53.9 (5)	51.3 (5)	54.8 (3)	53.5 (5)	53.8 (3)	53.4 (7)	50.7 (3)
Ce_2O_3	0.94 (13)	0.52 (7)	1.09	0.87 (12)	1.08 (11)	3.01 (42)	0.37 (11)	1.40 (7)	0.98 (8)	1.56 (17)	0.58 (47)
La_2O_3	0.62 (6)	0.25 (5)	0.45 (20)	0.46 (12)	0.58 (8)	1.57 (24)	0.14 (6)	0.71 (6)	0.43 (4)	0.81 (12)	0.34 (29)
SrO	0.75 (6)	0.58 (6)	0.30 (3)	0.34 (6)	0.70 (18)	0.86 (6)	0.32 (16)	0.30 (2)	0.40 (2)	0.56 (8)	1.35 (19)
Na_2O	<0.10	<0.10	<0.10	<0.10	<0.10	<0.10	<0.10	<0.10	<0.10	<0.10	1.95 (10)
P_2O_5	38.8 (6)	40.6 (4)	34.8 (2.0)	37.5 (6)	37.3 (9)	36.5 (1.7)	38.7 (6)	30.1 (6)	35.1 (1.0)	27.8 (2.7)	32.1 (1.2)
SiO_2	1.03 (19)	0.44 (18)	3.07 (1.0)	1.37 (24)	1.93 (39)	2.31 (39)	1.13 (25)	4.6 (2)	2.57 (23)	5.46 (1)	0.14 (22)
SO_3	0.25 (3)	0.20 (6)	0.53 (7)	0.30 (9)	0.35 (9)	0.29 (9)	0.45 (18)	0.79 (6)	0.63 (8)	0.85 (33)	2.02 (30)
CO_2[a]	0.72	0.12	1.29	1.08	1.04	0.63	0.87	3.14	1.24	3.93	n.c.
F	1.46 (15)	1.81 (42)	0.60 (18)	1.18 (15)	1.26 (25)	1.82 (75)	0.93 (15)	0.55 (7)	0.77 (21)	0.64 (35)	4.36 (19)
Cl	0.02 (5)	0.02 (1)	0.18 (7)	0.10 (1)	0.17 (2)	<0.02	0.20 (10)	0.15 (3)	0.14 (2)	0.12 (9)	0.15 (3)
OH[b]	1.99	1.69	2.65	2.18	2.11	1.58	2.42	2.74	2.49	2.67	n.c.
Total	100.08	100.33	98.26	99.08	100.42	99.87	100.33	97.98	98.55	97.80	93.69
O=F+Cl+OH	1.55	1.56	1.54	1.54	1.56	1.51	1.57	1.56	1.53	1.55	n.c.
Atomic relations calculated on the basis of 10 (Ca+Ce+La+Sr)											
Ca	9.828	9.894	9.872	9.881	9.827	9.619	9.937	9.837	9.870	9.795	9.173
Ce	0.059	0.033	0.069	0.056	0.067	0.193	0.023	0.088	0.063	0.098	0.036
La	0.039	0.016	0.029	0.029	0.036	0.101	0.009	0.045	0.028	0.051	0.021
Sr	0.075	0.057	0.030	0.034	0.069	0.087	0.032	0.030	0.040	0.056	0.132
Na	n.c.	n.c.	n.c.	n.c.	n.c.	n.c.	n.c.	n.c.	n.c.	n.c.	0.638
P	5.624	5.871	5.095	5.470	5.383	5.407	5.549	4.373	5.174	4.036	4.589
Si	0.177	0.075	0.531	0.236	0.329	0.404	0.192	0.789	0.448	0.936	0.024
S	0.032	0.026	0.069	0.038	0.045	0.038	0.057	0.102	0.081	0.109	0.026
C	0.166	0.028	0.305	0.256	0.242	0.151	0.202	0.738	0.295	0.920	n.c.
F	0.791	0.977	0.328	0.642	0.679	1.007	0.499	0.299	0.425	0.347	2.323
Cl	0.006	0.006	0.053	0.028	0.049	0.015	0.058	0.044	0.041	0.035	0.043
OH	1.198	1.019	1.169	1.332	1.269	0.977	1.444	1.055	1.534	1.617	n.c.
O	23.893	23.983	23.666	23.813	23.787	23.889	23.848	23.362	23.710	23.204	n.c.

[a] Calculated based on P+Si+S+C=6 assuming ideal stoichiometry, also verified by coulometric titration
[b] Calculated based on F+Cl+OH=2 assuming ideal stoichiometry
n.c. Not calculated
[ ] Number of averaged analyses
( ) Standard deviation showing the last significant digits
< Below minimum detactable limit
Sample 219 (not listed here) is very similar in composition to sample 5/12

1,410 cm^{-1} was made in order to understand the way CO_2 enters the apatite structure and to see possible effects of fluid inclusions.

Results

The compositional characteristics and the substitution mechanism of the Kaiserstuhl apatites are exhibited by the pronounced chemical variations found. A selection of representative electron microprobe analyses of apatites from a variety of carbonatites and some silicate rock types is compiled in Table 1. The analyses have been recalculated assuming that proper stoichiometry is maintained. This assumption is well supported by the synthetic growth of crystallized carbonate fluorapatite and carbonate hydroxyapatite of accurately represented apatite stoichiometry (Jahnke 1984). Thus the atomic numbers have been normalized on the basis of 10 A-site cations according to the general apatite formula which is expressed as:

$$A_{10}(XO_4)_6\,Z_2$$

Where A = Ca^{2+} and medium to large cation substituents which may occupy 2 lattice sites with VII- and IX-fold coordination (Ca_{II} and Ca_I)
X = P^{5+} and small cation substituents with tetrahedral coordination
Z = halogenides (F^-, Cl^-) and OH^-

In the apatite structure (Beevers and McIntyre 1946; Posner et al. 1958), a number of substituting ions with specific ionic radii and respective coordination numbers are reported to occupy the three major structural sites. Crystal-chemical discussions are found summarized in Liebau (1966), McConnell (1973) and Roy et al. (1978). Potential substit-

Table 1b. Electron microprobe analyses of apatites from various silicate magmatites. Mean and standard deviation

	Shonkinite porphyry Horberig [10]	Phonolitic dyke Boetzingen [17]	Phonolitic tuff Limberg [11]	Tephrite dyke 435 [3]	Bergalite cpx-rich 340 [4]	Bergalite 217 [5]
CaO	54.2 (7)	54.3 (3)	53.9 (7)	54.9 (3)	53.1 (4)	54.1 (6)
Ce_2O_3	0.39 (24)	0.41 (16)	0.71 (24)	0.33 (4)	0.49 (9)	0.43 (16)
La_2O_3	0.17 (15)	0.20 (10)	0.38 (23)	0.18 (4)	0.28 (5)	0.18 (7)
SrO	0.51 (23)	0.53 (27)	0.92 (20)	0.60 (7)	0.85 (15)	0.54 (4)
P_2O_5	39.4 (7)	39.7 (7)	38.1 (1.6)	40.8 (25)	39.4 (7)	38.7 (1)
SiO_2	0.70 (26)	0.54 (34)	1.33 (61)	0.54 (16)	0.93 (9)	1.55 (43)
SO_3	0.67 (35)	0.63 (41)	0.49 (26)	0.45 (19)	0.41 (20)	0.79 (20)
CO_2[a]	0.39	0.43	0.93	0.10	0.0	0.10
F	1.50 (49)	2.14 (56)	2.15 (39)	2.13 (12)	3.45 (11)	1.58 (18)
Cl	0.46 (11)	0.26 (14)	0.11 (12)	1.01 (5)	0.04 (8)	0.14 (8)
OH[b]	1.75	1.29	1.34	0.96	0.16	1.84
Total	100.13	100.48	100.25	101.98	99.13	99.96
O=F+Cl+OH	1.56	1.56	1.56	1.58	1.54	1.56
Atomic relations calculated on the basis of 10 (Ca+Ce+La+Sr)						
Ca	9.914	9.910	9.843	9.910	9.865	9.908
Ce	0.024	0.025	0.044	0.020	0.031	0.027
La	0.011	0.013	0.022	0.011	0.018	0.011
Sr	0.051	0.052	0.091	0.059	0.085	0.054
P	5.702	5.730	5.495	5.829	5.782	5.609
Si	0.118	0.092	0.227	0.091	0.161	0.265
S	0.086	0.080	0.061	0.067	0.053	0.101
C	0.091	0.100	0.217	0.023	0.0	0.024
F	0.810	1.153	1.160	1.136	1.891	0.855
Cl	0.133	0.072	0.032	0.289	0.012	0.041
OH	1.058	0.776	0.807	0.572	0.098	1.112
O	23.948	23.970	23.842	23.989	23.999	23.948

[a] Calculated based on P+Si+S+C=6 assuming ideal stoichiometry, also verified by coulometric titration
[b] Calculated based on F+Cl+OH=2 assuming ideal stoichiometry
[ ] Number of averaged analyses
( ) Standard deviation showing the last significant digits
< Below minimum detectable limit

uent elements in the apatite structure were examined according to the ionic radii taken from Shannon and Prewitt (1969). A survey of the chemical constituents in the apatites from the Kaiserstuhl rocks showed that only a few are present in significant concentrations.

The alkaline-earth elements Na and K exhibit low concentrations, virtually below 0.1 wt.%. Apatites with Na_2O enrichments of up to 2 wt.% are observed which, however, can be attributed to trapped phosphate melt inclusions in apatites from comb-layer alvikites such as sample 11/17 (Sommerauer and Katz-Lehnert 1985).

Irrespective of rock type, the following elements were found to be close to the individual MDL and never exceeding 0.1 wt.%. These are Al, Mg, V, Fe, Ni, Cr, and Th. Therefore, their presence has little significance for the crystal chemistry of the Kaiserstuhl apatites. Also there is essentially no Ti, Ba, Mn, and Nb detectable in any of the apatite samples (with an MDL of about 200 to 500 ppm), even though the carbonatites are enriched in Ba, Mn, and Nb (Katz-Lehnert, in prep).

In contrast to this, distinct chemical patterns and mutual relationships are revealed by the major elements Ca, P, F, and the principal substituents Si, C, Sr, LREE, S, and Cl. They will be discussed below with respect to the substitution sites available, and in accordance with their ionic radii.

The averaged composition and the appropriate standard deviation of each apatite sample (Table 1) yield a pronounced chemical variation inherent to the samples analyzed even though the composition within the single crystals is generally very homogeneous. An exception from this are the apatites from a porphyric alvikite (sample 11/29) which are distinctly zoned.

On the basis of the electron microprobe data (Table 1), it is evident that the apatite specimens investigated are best described as Hydroxyapatite, covering a wide compositional range reflected by the prominent substituents Si, C, LREE, and F. The chemical characteristics of these hydroxyapatites are consistent with the x-ray powder data of some apatite samples. The calculated cell constants (Table 2) are in excellent agreement with those from hydroxyapatite or from dahlite (a carbonate-hydroxy-apatite), both of which have similar cell parameters. The silicate-apatites, ellestadite and wilkeite, may be positively ruled out because of the cell constants. The apatites analyzed in this work revealing positively correlated amounts of Si and C shall be subsequently referred to as silicate-carbonate-hydroxy-apatite (SCHap).

Table 2. Lattice constants of some Kaiserstuhl carbonatite apatites and, for comparison, those of Hap, Fap, dahlite, and francolite

	a	c	Comp.	Reference
G004	9.3740 (14)	6.8833 (17)	Fap std.	this work
5/12	9.4132 (11)	6.8916 (13)	Hap+Si,C	this work
11/29	9.4126 (11)	6.8922 (14)	Hap+Si,C	this work
11/17	9.4110 (30)	6.9063 (30)	Hap+Si,C	this work
Hap	9.418	6.884	synth.	ASTM 9–432
Fap	9.3684	6.8841	synth.	ASTM 15–876
Dahlite	9.419	6.89	Hap+C	McConnell (1973)
Francolite	9.36	6.90	Fap+C	McConnell (1973)

( ) 1 sigma standard deviation
Fap Fluorapatite
Hap Hydroxyapatite

Substitution in the A-position (Ca^{2+}, Sr^{2+}, REE^{3+})

Sr^{2+} and the REE^{3+} are considered to be the only major ions to replace Ca^{2+} as there is a distinct antipathetic relationship between the sum of Sr+REE and the Ca content. Other possible substituting elements are K, Na, Mg, and Th, which only occur in low level concentrations as mentioned previously.

Of the REE, only Ce and La were quantitatively determined by means of electron microprobe techniques. Small amounts of Nd were detected with concentrations of approximately 1/10 to 1/3 of the amount of La present. The REE analyses reveal a pattern with strong enrichment of the light REE (LREE). These results are in good agreement with the NAA results of selected apatite samples (5/12 and 11/29). They are, however, in marked contrast to the observation by Puchelt and Emmermann (1976) who described a characteristic negative Ce (and Eu) anomaly.

Considering the substitution of $LREE^{3+}$ for Ca^{2+} ion, it is obvious that the resulting more positive charge must be balanced by either an A^{1+} ion or by equivalent coupled compensation of other site substituents. In the absence of adequate concentrations of A^{1+}, charge balance is confined to either O^{2-} in the Z-site or more realistically to substituting ions in the X-site (e.g. CO_3OH^{3-}, SiO_4^{4-}), see below.

Substitution in the XO_4-position (P^{5+}, Si^{4+}, C^{4+}, S^{6+})

Likely substituents for the tetrahedrally coordinated PO_4^{3-} group are SiO_4^{4-} and SO_4^{2-}. While SiO_2 is present in moderate to high concentrations, SO_3 is low, approximately 1/10 of the SiO_2 concentration (Table 1). P_2O_5 exhibits a wide concentration range, pointing to extensive substitution in this site. In fact, a decrease in P_2O_5 is closely correlated to an increase of SiO_2. This is shown in Fig. 1 where Si is plotted with respect to P from the apatite samples investigated. The least square linear regression yields a pronounced deficiency in the X-site occupation with increasing Si concentration; while 2 P atoms become apparently vacant, only 1 Si atom enters the X-site. Thus, an equal number of atoms of another element or a sum of elements (X_i) including S is required to maintain the structural balance (Fig. 1), which amount is given by:

$$m*\sum(X_i)+m*(Si)=2*m(P) \quad \text{where } m=\text{number of atoms.}$$

In order to explain the observed deficiency in the X-site occupancy, light elements not easily detectable by means of the electron microprobe have been examined. Carbon has been identified and semiquantitatively analyzed in specially prepared samples. Based on the assumption that carbon might enter the tetrahedral site as a CO_3^{2-} group in the apatite structure (see discussion), carbon was stoichiometrically calculated for each analysis to assure 6 X-site atoms in total (Table 1). These results have been qualitatively confirmed by IR spectroscopic data of the C–O absorption band which appears in both samples 5/12 and 11/29. In the latter it is stronger developed and is consistent with the higher C concentration. The C–O vibration between 1,410 and 1,470 cm^{-1} is clearly splitted unlike the C–O absorption band of calcite which is in agreement

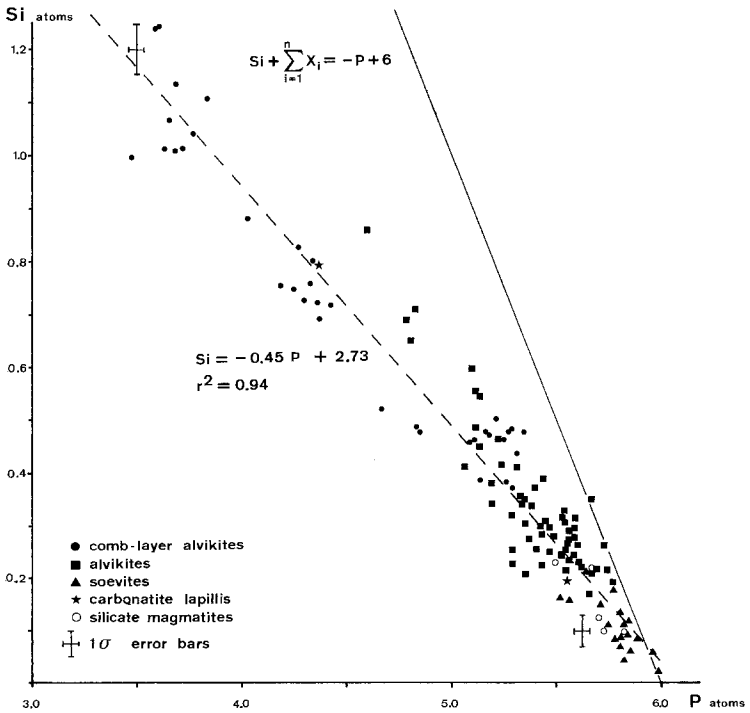

Fig. 1. Si plotted versus P in atomic numbers normalized to 10 A-site atoms of apatites from selected carbonatites and silicate magmatites of the Kaiserstuhl igneous complex (131 electron microprobe data points). r^2 is the coefficient of determination of the least square linear regression

Table 3. CO_2 determination by coulometric titration and results by stoichiometric computation from electron microprobe data of apatite concentrates from carbonatites and one CO_2-free apatite standard (G_{005})

	CO_2 calc.	CO_2 analyzed
5/12	1.1 (0.1)	1.2 (0.02)
11/29	1.3 (0.5)	1.7 (0.03)
G005	0.0	0.0

( ) Standard deviation

with Gulbrandsen et al. (1966) and Brophy and Nash (1968) thus excluding calcite as responsible for this C–O vibration. Coulometric titration yielded carbon contents in good agreement with the stoichiometrically estimated CO_2 concentrations. Averaged carbon concentrations evaluated by the stoichiometric method together with the quantitative determinations based on the coulometric titration are found in Table 3 for two representative samples and one apatite standard. As concluded by the coulometric titration results (see methods) and the IR C–O absorbtion data, carbon occurs most probably as CO_2^{3-} group in the apatite structure. Elemental carbon may be discredited. Calcite as the source for the carbon signal may also be ruled out. However, fluid inclusions containing some CO_2 may attribute to the total carbon oxide measured by the coulometric titration method.

Substitution in the Z-position (F^-, OH^-, Cl^-)

Fluorine covers a wide compositional range (Fig. 2), though distinctly less than 2.5 wt.% (Table 1). Cl concentrations in apatites from carbonatites are generally low and may occasionally reach 0.20 wt.%. Apatites from most of the silicate rocks have characteristically higher Cl concentrations (Fig. 2) and in several cases, may show enrichments of up to 2 wt.%. Thus the major component of the Z site is hydroxyl (OH) which was determined stoichiometrically based on the assumption that $2-(F+Cl)=OH$. Hydroxyapatite has been further confirmed by IR spectroscopy which shows distinct O–H vibrations and by the x-ray powder results (Table 2), where a significant spread in the cell dimensions between OH-apatite (Hap) and F-apatite (Fap) is observed.

Young and Munson (1966) found O^{2-} to be a possible substituent in natural occurring apatites. Even though O^{2-} may be considered a likely substituent thus accounting for charge balance in this site, this seems to be of minor importance due to an excess negative charge balance in the Schap formula found.

Discussion

The incorporation of carbon in the apatite structure

An inherent problem of carbonate-apatites in general is the distinct discrepancy in which manner carbon is incorporated in the apatite structure. Since McConnell and Gruner (1940) concluded that carbonate-apatites are not to be explained on the basis of contamination by $CaCO_3$, there has been no doubt about the entry of carbon into the apatite structure. Regarding the ionic radii, it is not likely that carbon substitutes for A-site ions as suggested by McConnell (1937) or that carbon is equally shared by the A- and X-sites, respectively (McConnell 1938). On the other hand, a substitution for the halogenides (Z-site) as suggested by McConnell and Gruner (1940) has been subsequently discredited by McConnell (1952) and Trueman (1966). Based on X-ray studies of synthetic carbonate-apatite, LeGeros (1965) ruled out substitution of carbonate for the hydroxyl group and favored instead the substitution of a CO_3^{2-} group for PO_4^{3-}. This was confirmed by Eysel and Roy (1973) from IR studies. McConnell (1952) postulated a substitution mechanism similar to $3\ PO_4^{3-}=4\ CO_3^{2-}$ which would require corresponding partial absence of Ca, presumably replaced by OH, H_2O, or H_3O. McClellan and Lehr (1969) disproved this model based on a series of apatite analyses exhibiting a substitution ratio of 1/1 for PO_4/CO_3. Results of the present work give evidence that approx. one CO_3^{2-} + one SiO_4^{4-} replace two PO_4^{3-} as plotted in Fig. 3 neglecting the minor effect of SO_4^{2-}. No simple correlation could be found between the carbon concentration and the Z-site or A-site atoms, respectively, which excludes a systematic carbon substitution mechanism for these sites.

Stadler (1981) yet found evidence for both the X- and the Z-substitution mechanism for CO_3^{2-}, with preference for the tetrahedral site substitution. According to Stadler, this mechanism is accompanied by a Ca deficiency and coupled hydroxyl occupation. As suggested by McConnell (1938) carbon may enter the apatite structure as a planar triangular CO_3^{2-} group replacing the tetrahedral PO_4^{3-}. This was confirmed by Stadler (1981) based on infrared spectroscopy showing that such type of group is tilted with respect to the hexagonal screw axes thereby leaving one O^{2-} vacant and in turn decreasing the total charge due

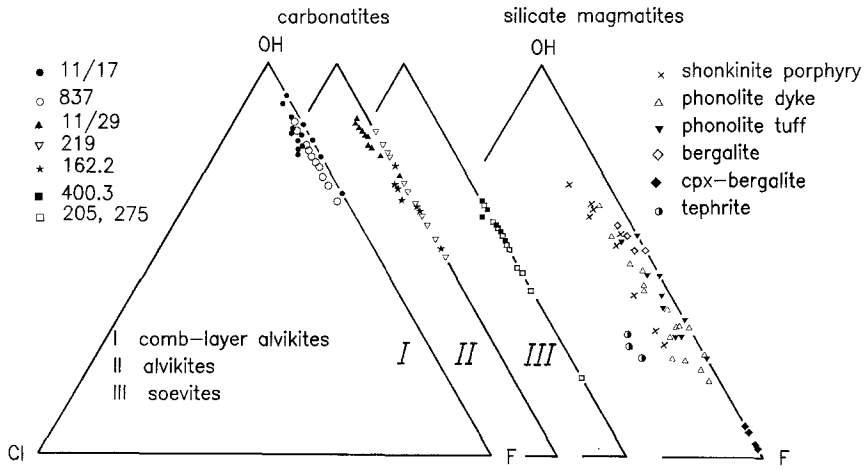

Fig. 2. Triangular plot of the halogenides in atoms normalized to 10 A-site atoms of apatites from selected carbonatites and silicate magmatites of the Kaiserstuhl igneous complex. The number of data points of each apatite sample are found in Table 1

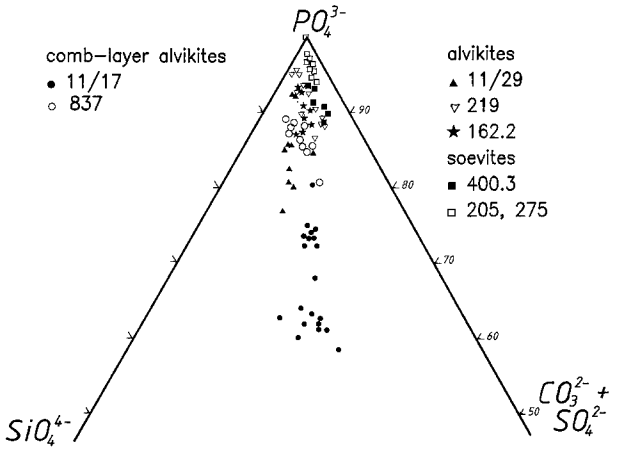

Fig. 3. Triangular plot of the tetrahedral site ions in atomic numbers normalized to 10 A-site atoms of apatites as in Fig. 1 with SiO_4^{4-} and $CO_3^{2-}+SO_4^{2-}$ compared to the substituted PO_4^{3-} group. They are grouped with respect to charge

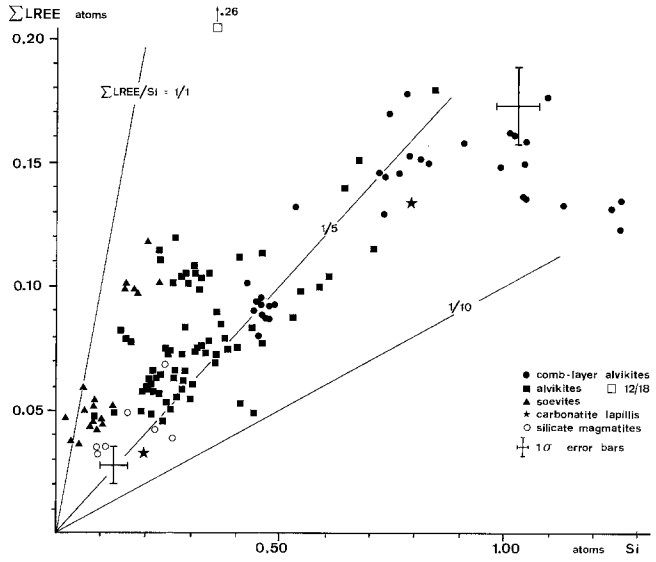

Fig. 4. LREE represented by Ce+La as major componets platted versus Si in atomic numbers normalized to 10 A-site atoms of apatites as in Fig. 1. An almost linear progressive relationship occurs between LREE and Si with a LREE/Si ratio distinctly less than 1/1 and averaging 1/5

to partial replacement of the PO_4^{3-} ion. Borneman-Starinkevich and Belov (1953) advanced the idea that when a CO_3^{2-} ion substitutes for a tetrahedral phosphate group, the vacant oxygen site would be occupied by a fluorine ion expressed as CO_3F^{3-}. Trueman (1966) substantiated this mechanism by plotting the halogenides and OH in function of carbon suggesting groups such as CO_3F^{3-} and CO_3OH^{3-}. This kind of substitution mechanism is appealing in that carbon is truly tetrahedrally coordinated and that no charge imbalance is produced during progressive replacement of PO_4^{3-} groups. Gulbrandsen et al. (1966) assumed likewise a substitution of CO_3^{2-} and F^{1-} for the PO_4^{3-} group coupled to a balanced pair of $LREE^{3+}$ and Na^{1+} substitution for Ca^{2+}. A coupled substitution of Na^{1+} and CO_3^{2-} is disproved by Stadler (1981) on the basis of infrared spectroscopy and may be ruled out for the Kaiserstuhl apatites by the results of this work since Na is always below detection limit (Table 1). A negatively correlated and curvilinear relationship has been found between SiO_2 and F and hence between CO_2 and F. This precludes the existence of a CO_3F^{3-} group, conversely favouring CO_3^{2-} and/or CO_3OH^{3-} as potential substitutional groups.

Since SiO_4^{4-} is progressively correlated with $CO_3^{2-}+SO_3^{2-}$, characterized by a ratio of practically 1 to 1 as shown in Fig. 3, charge balance in situ is provided. For this substitution there is no need for a charge balance using the hypothetical group CO_3OH^{3-}. However, charge balance is required regarding the $LREE^{3+}$ substituting Ca^{2+}. A possible mechanism appears to exist between SiO_4^{4-} and $LREE^{3+}$ based on a positive correlation of their concentration as depicted by Fig. 4. Furthermore Watson and Green (1981) found the substitution mechanism $REE^{3+}+Si^{4+} <-> Ca^{2+}+P^{5+}$. Yet the atomic ratio of LREE/Si in this investigation varies around 1/5 and is far from 1/1 which would be required for the substitution mechanism proposed. Thus in the case of the Kaiserstuhl apatites, this compensation can not be the dominating mechanism. Charge compensation for $LREE^{3+}$ is more likely to be attributed to CO_3OH^{3-} and consequently the ratio of CO_3OH^{3-} to CO_3^{2-} may be related to the amount of LREE present. If this is true, it is likely that the LREE occupy preferentially the Ca_{II} site which is coordinated by one OH or F ion and six oxygens (Sudarsanan and Young 1978). One would expect, therefore, that the LREE in the apatite structure would have an ordering effect on the two Ca sites. Unfortunately the x-ray data do not exhibit such a mechanism. Lacking a distinct mineral-chemical substition mechanism of the LREE in the apatites analyzed, the incorporation of LREE is believed to be primarily controlled by geochemical processes and therefore by the chemical fractionation of the magma involved (Katz-Lehnert and Sommerauer, in prep).

The substitution mechanism of PO_4^{3-} with SiO_4^{4-} and CO_3^{2-}

The compositional correlations of CO_2, SiO_2, and P_2O_5 are very pronounced and the wide range of chemical compositions (Table 1) suggests a new partial apatite solid solution series. The major characteristics are manifested in Fig. 3 by the paired substitution of $1\ SiO_4^{4-}+1\ CO_3^{2-}=2\ PO_4^{3-}$. Disregarding the incorporation of LREE and the possible CO_3OH^{3-} group this hydroxyapatite series may be expressed as follows:

$$Ca_{10}(SiO_4)_x(CO_3)_x(PO_4)_{6-2x}(OH, F)_2$$

with $0<x<1.2$ as observed.

This proposed relationship is substantially confirmed by the X-ray powder data (Table 2). The cell constants a_0 and c_0 are plotted as a function of F, P_2O_5, and SiO_2, respectively, in Fig. 5. Wheras the cell constants are clearly independent of the F concentration, they are not so in the case of P_2O_5 and SiO_2. It is evident that Sr as a substituent for Ca is not abundant enough to produce significant changes. Furthermore, Sr is fairly constant and thus cannot be responsible for the observed variations of the cell constants. However, the $LREE^{3+}$ might have some influence on both a_0 and c_0 due to a larger ionic radius than Ca^{2+}. This may be manifested by larger cell constants of synthetic apatite species (Mayer et al. 1974) and by natural apatites, e.g. beckelite, lessingite, britholite, respectively. The fact that c_0 increases while a_0 decreases with progressively depleted P_2O_5 concentrations (Fig. 5) excludes a primary effect of the LREE and favours instead the dependence of the cell constants on SiO_4^{4-} and, due to the paired substitu-

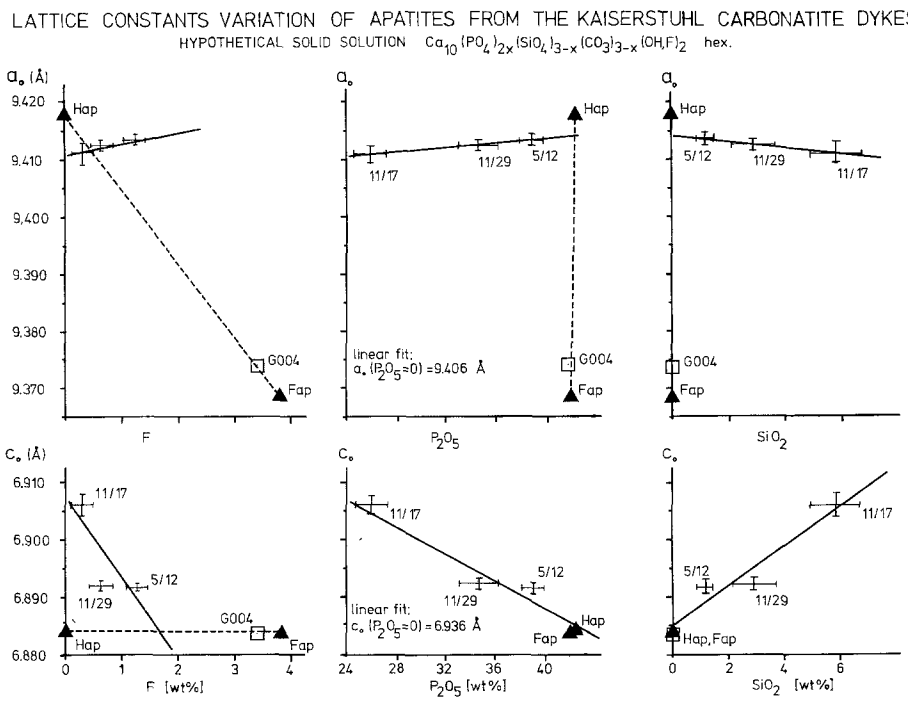

Fig. 5. Lattice constants of selected apatite samples from carbonatites in function of F, P_2O_5, and SiO_2, respectively. Full triangles represent cell constants of hydroxyapatite (Hap) and of fluorapatite (Fap). G004 is a natural apatite reference standard with a composition close to Fap. The continuous lines represent least square linear regressions

tion of PO_4^{3-} with CO_3^{2-} (Fig. 3) and/or CO_3OH^{3-}, an inherent effect of carbon concentration on the cell constants. The mean P–O distance is 1.53Å in hydroxyapatite (Posner et al. 1958). Tetrahedrally coordinated SiO_4^{4-} has a Si–O distance of about 1.67 Å due to the larger Si^{4+} (after Shannon and Prewitt 1969). In calcite a planar triangular CO_3 group has a C–O distance of 1.29 Å (Saas et al. 1957). Comparing these cation-oxygen distances gives evidence that the cell constants will be more affected by the carbonate ion than by the SiO_4^{4-} group in replacement for the PO_4^{3-}. In fact, LeGeros (1965) found that a_0 contracts linearly with increasing substitution of phosphorous by the smaller, presumably tilted CO_3^{2-} groups with respect to the PO_4^{3-} groups exchanged along the 6_3 axes, whereas c_0 appears to be virtually equal in size to that of hydroxyapatite. The c_0 cell values exhibited in Fig. 5 however are significantly larger compared to c_0 of hydroxyapatite. Thus it is concluded that a mutual increase of SiO_2 and LREE might be responsible for an expansion of the cell constant, c_0.

Except for F, there are well established linear relationships of the cell constants with the amount of phosphorous, and with silicon as shown in Fig. 5. Extending the linear relationship to a hypothetical end-member with P totally substituted, the resulting SiO_2 and CO_2 concentrations are in good agreement with values derived by stoichiometric computation. Based on this well substantiated substitution mechanism it is proposed that this new series is referred to as silicate-carbonate-hydroxyapatite (SCHap). A similar apatite series has been reported with a substitution of 1 SO_4^{2-} and 1 SiO_4^{4-} for 2 PO_4^{3-} (McConnell 1937; Rouse and Dunn 1982).

In contrast to the chemical characteristics mentioned there is a non-linear relationship between LREE and F. This is incompatible with control by a crystal-chemical substitution mechanism but is thought to reflect geochemical constraints. Nash (1972) interpreted the increasing F concentration in apatite from a carbonatite from Iron Hill (Colorado) as due to progressive differentiation of the host rocks. On the basis of the experiments in the system CaO–CaF_2–P_2O_5–H_2O (Biggar 1967) hydroxyapatite seems to be the common primary apatite in igneous rocks and that fluorine is incorporated in relation to decreasing pressure. In accordance with this, the Kaiserstuhl carbonatite apatite formation is interpreted as a consequence of rock evolution, the F-rich hydroxyapatite from soevites being more evolved than the almost F-free apatites from quenched (comb-layer) alvikite (Fig. 2) which are considered the direct precipitate of the late stage melt (Katz-Lehnert and Sommerauer, in prep). This relationship is well demonstrated by the chemical variation of the halogenides in the different apatite samples from the carbonatite and from the silicate rocks plotted in Fig. 2. The similarity of the compositional range of the apatites from the carbonatites and the associated silicate rock types (Table 1, Fig. 2) exhibits the close petrogenetic relationship of the rock types from the Kaiserstuhl alkaline volcanic complex.

Conclusions

1. The compositional range of the apatites analyzed reveal an extended paired substitution of PO_4^{3-} with SiO_4^{4-} and CO_3^{2-}/CO_3OH^{3-}. Up to about 60% of the X-site is found to be substituted by silicon and carbon. It is assumed that a complete solid solution series of silicate-carbonate-hydroxyapatite might be realized in nature.

2. Carbon enters the investigated silicate-carbonate-hydroxyapatite as CO_3^{2-} and/or as CO_3OH^{3-} group replacing the tetrahedral PO_4^{3-}. The portion of the two carbonate groups incorporated is essentially dependent on the LREE substituted for Ca providing the required charge balance.

Acknowledgements. We are deeply indebted to B.W. Evans, E.H. Perkins, and to B.W.D. Yardley for critically reading the manuscript and for their constructive comments. The reviewer Mrs. H.C. Skinner is greatly acknowledged for her thorough reading and very valuable suggestions. Thanks are given to E. Schaerli and A. Willi for preparing the electron microprobe samples. We are grateful to V. Dietrich and M. Amgwerd for carrying out the coulometric titration, A. Wyttenbach for the neutron activation analyses, A. Rub for doing the combined differential thermal analysis and mass-

spectrometry, M. Wennemer for recording the x-ray diffraction patterns, and G. Brunner for taking some IR spectras. All of the interesting discussions with colleagues are gratefully acknowledged. We thank J. Keller who has contributed valuable discussions. One of us (K. Katz-Lehnert) acknowledges the financial support from the German N.F.

References

Axelrod S, Rohrlich V (1982) Chemical variability in francolites from Israeli phosphorites macrograins. Mineral Deposita 17:1–15

Beevers CA, McIntyre DB (1946) The atomic structure of fluorapatite and its relation to that of tooth and bone material. Mineral Mag 27:254–257

Belyakov AYu, Kravchenko SM (1979) The distribution of rare earths in apatite as an indicator of the basicity and origin of comagmatic rock series. Trans from Doklady Akademii Nauk SSSR. 248/5:1216–1220

Biggar GM (1967) Apatite compositions and liquidus phase relationships on the join $Ca(OH)_2-CaF_2-Ca_3(PO_4)_2-H_2O$. Mineral Mag 36:539–564

Borneman-Starinkevich ID, Belov NV (1953) Carbonate-apatites. Dokl Adad Nauk SSSR 90:89–92

Brophy GP, Nash TJ (1968) Compositional, infrared and X-ray analysis of fossil bone. Am Min 53:445–454

Daub R (1912) Beiträge zur Kenntnis der Kontaktmineralien aus dem körnigen Kalke des Kaiserstuhls. Inaug Diss, Freiburg i Br

Eysel W, Roy DM (1973) Hydrothermal flux growth of hydroxyapatites by temperature oscillation. J Crystal Growth 20:245–250

Gubser R, Sommerauer J (1977) EMMA, Correction Procedure for Quantitative Electron Probe Analyses. ETHZ, unpublished

Gulbrandsen RA, Kramer JR, Beatty LB, Mays RE (1966) Carbonate-bearing apatite from Faraday Township, Ontario, Canada. Am Mineral 51:819–824

Ito J (1968) Silicate apatites and Oxyapatites. Am Mineral 53:890–907

Jahnke RA (1984) The synthesis and solubility of carbonate fluorapatite. Am J Science 284:58–78

Katz K, Keller J (1981) Comb-layering in carbonatite dykes. Nature 294:350–352

Katz-Lehnert K (1985) Doctoral thesis, University Freiburg i Br (in prep)

Katz-Lehnert K, Sommerauer J (1985) The formation of silicate-carbonate-hydroxyapatite and its relation to the carbonatite rock evolution of the Kaiserstuhl (SW-Germany) (in prep)

Keller J (1981) Carbonatitic Volcanism in the Kaiserstuhl alkaline complex: evidence for highly fluid carbonatitic melts at the earth's surface. J Volcanol Geotherm Res 9:423–431

LeBas MJ, Handley LD (1979) Variation in apatite composition in ijolitic and carbonatitic igneous rocks. Nature 297:54–56

LeGeros RZ (1965) Effect of carbonate on the lattice parameters of apatite. Nature 206:403–404

Liebau F (1966) Die Kristallchemie der Phosphate. Fortschr Mineral 42:266–302

Manheim FT, Gubrandsen RA (1979) Marine phosphorites. From: Marine Minerals, 6, R.G. Burns, Short Course Notes, 151–173. Mineral Soc Am Washington, DC

Mayer I, Roth RS, Brown WE (1974) Rare earth substituted fluoride-phosphate apatites. J Solid State Chem 11:33–37

McClellan GH, Lehr J (1969) Crystal-chemical investigation of natural apatites. Am Mineral 54:1374–1391

McConnell D (1937) The substitution of SiO_4- and SO_4-groups for PO_4-groups in the apatite structure; ellestadite, the end-member. Am Mineral 22:977–986

McConnell D (1938) A strucktural investigation of the isomorphism of the apatite group. Am Mineral 23:1–19

McConnell D (1952) The problem of the carbonate apatites. IV. Structural substitutions involving CO_3 and OH. Bull Soc Fr Mineral Cryst 75:428–445

McConnell D (1973) Apatite, its Crystal Chemistry, Mineralogy, Utilization, and Geology and Biologic Occurences. Springer, Berlin Heidelberg New York Tokyo

McConnell D, Gruner JW (1940) The problem of the carbonate-apatites. III. Carbonate-apatite from Magnet Cove, Arkansas. Am Mineral 25:157–167

Nash WP (1972) Apatite-calcite equilibria in carbonatites: chemistry of apatite from Iron Hill, Colorado. Geochim Cosmochim Acta 36:1313–1319

Posner AS, Perloff A, Diorio AF (1958) Refinement of the hydroxyapatite structure. Acta Cryst 11:308

Prins P (1973) Apatites from African carbonatites. Lithos 6:133–144

Puchelt H, Emmermann R (1976) Bearing of rare earth patterns of apatites from igneous and metamorphic rocks. Earth Planet Sci Lett 31:279–286

Rouse RC, Dunn PJ (1982) A contribution to the crystal chemistry of ellestadite and the silicate sulfate apatites. Am Min 67:90–96

Roy DM, Drafall E, Roy R (1978) Crystal chemistry, crystal growth, and phase equilibria of apatites. From: Phase Diagrams. Material Sciences and Technology, Vol. 6-V, A.M. Alper, Academic Press, New York, pp 185–239

Saas RL, Vidale R, Donohue J (1957) Interatomic distances and thermal anisotropy in sodium nitrate and calcite. Acta Cryst 10:567

Shannon RD, Prewitt CT (1969) Effective Ionic Radii in Oxides and Fluorides. Acta Cryst B25:925–945

Sixta V (1977) Coulometric determinations of carbonates in rock samples. Z Anal Chem 285:369–372

Sommerauer J (1981) COMIC-ED Manual: Control and Data Acquisition Program for the Microprobe SEMQ (ARL). ETHZ, unpublished

Sommerauer J, Katz-Lehnert K (1985) Trapped phosphate melt inclusions in silicate-carbonate-hydroxyapatite from quenched alvikite dykes from the Kaiserstuhl carbonatite complex (W-Germany) Contrib Mineral Petrol 91:281–286

Stadler HJ (1981) Beiträge zur Kenntnis der Carbonat-Apatite. Dissertation Universität Karlsruhe (57 pages)

Sudarsanan K, Young RA (1978) Structural interactions of F, Cl and OH in apatites. Acta Cryst B34:1401–1407

Taborszky FK (1962) Geochemie des Apatits in Tiefengesteinen am Beispiel des Odenwaldes. Beitr Mineral Petrogr 8:354–392

Trueman NA (1966) Substitutions for phosphate ions in apatite. Nature 210:937–938

Van Wambecke L (1964) Geochemie minerale des carbonatites du Kaiserstuhl. From: Les roches alcalines et les carbonatites du Kaiserstuhl. EURATOM, Rapport 1827. d,f,e, Bruxelles, 232 pages

Walther J (1981) Fluide Einschlüße im Apatit des Karbonatits vom Kaiserstuhl. Ein Beitrag zur Interpretation der Karbonatitgenese. Dissertation Universität Karlsruhe (195 pages)

Watson EB, Green TH (1981) Apatite/liquid partition coefficients for the rare earth elements and strontium. Earth Planet Sci Lett 56:405–421

Wimmenauer W (1957) Beiträge zur Petrographie des Kaiserstuhls, Teil I. N Jahrb Mineral Abh 91:131–150

Wimmenauer W (1959) Beiträge zur Petrographie des Kaiserstuhls, Teile I (Schluß), II, III. N Jahrb Mineral Abh 93:137–173

Wimmenauer W (1962) Beiträge zur Petrographie des Kaiserstuhls, Teile IV, V. N Jahrb Mineral Abh 98:367–415

Wimmenauer W (1963) Beiträge zur Petrographie des Kaiserstuhls, Teile VI, VII. N Jahrb Mineral Abh 99:231–276

Wimmenauer W (1967) Igneous rocks in the Rhinegraben. In: The Rhinegraben Progress Report 1967. Rothe JP, Sauer K, Freiburg i.Br./Strasbourg, 144–148

Young EJ, Munson EL (1966) Fluor-Chlor-Oxy-Apatite and Sphene from Crystal Lode Pegmatite near Eagle, Colorado. Am Mineral 51:1476–1493

Received January 28, 1985 / Accepted June 27, 1985